PAPER

CrossMark
← click for updates

Improved properties of bidispersed magnetorheological fluids

Mahesh Chand, Ajay Shankar, Noorjahan, Komal Jain and R. P. Pant*

We have investigated the influence of nanosized particle concentration on rheological properties when mixed with a magnetorheological (MR) fluid. We have also studied the structural, morphological and magnetic properties of ferrofluid-based MR fluids (F-MRFs). Field-induced rheological and viscoelastic properties of F-MRFs with varying shear rate and strain amplitude have been investigated. The Herschel–Bulkley model was found to fit well with the flow behaviour of F-MRFs. In the oscillatory strain sweep test, F-MRFs show linear viscoelasticity at low strain and the storage modulus (G') is higher than the viscous modulus (G''), which indicates the existence of strong links among the particles that form the microscopic structures. The storage modulus increases with increasing weight fraction of nanosized particles. Furthermore, the loss factor (ratio of G'' and G') was also investigated as a function of magnetic field strength. In addition, time-dependent relaxation behaviour of magnetically induced chain-like structures has also been described. The study reveals that the addition of nanoparticles to MR fluids increases the viscosity as well as the fluid stability under a magnetic field.

1. Introduction

MR fluids are systems in which micron-sized magnetic particles are dispersed in a non-magnetic medium. These are complex fluids and exhibit a remarkable change in their rheological properties under the influence of an external magnetic field.[1–4] The important characteristics of these fluids are yield stress, viscosity, and settling rate, which make them suitable for technical applications.[5–7] These properties can be tuned by optimizing the synthesis parameters and choosing the ingredients.[8–11] Some problems, such as particle aggregation and settling rate, affect the performance of MR fluid and restrict its use in applications.[12–14] To rectify these issues, different procedures have been adopted like addition of thixotropic agents or surfactants and use of viscoplastic media, but sometimes these processes hinder the MR effects. Recently, it was reported that the use of ferrofluid (FF) is an effective way to reduce the settling rate of micron-sized particles in MR fluid.[15–19] On the application of a magnetic field, the micron-sized particles become polarized and gather in chains or clusters due to dipole–dipole interaction. It is seen that formation of these clusters creates microcavities within the structures. These cavities are easily occupied by ferrofluid nanosized particles making a kind of colloidal nanobridge (CNB).[20–22] Thus, nanofluid-based MR fluid improves its stability and becomes more favorable for various applications like dampers, clutches, lubricants, and bearings.[23–30]

CSIR-National Physical Laboratory, Dr K S Krishnan Marg, New Delhi-110012, India. E-mail: rppant@nplindia.org

The present work deals with the preparation of MR fluids and further mixing with varying volume percentages of magnetite-based ferrofluid nanoparticles. Before carrying out magnetorheological investigations, the fluid mixture was investigated for its physical properties, like structural and magnetic properties, by X-ray diffraction (XRD), high-resolution transmission electron microscopy (HRTEM) and vibrating sample magnetometer (VSM) techniques. The effect of FF nanoparticles on the stability of such bidispersed MR suspensions has been investigated by examining viscoelastic measurements using a magnetorheometer at different field values.

2. Experimental

2.1 Materials and synthesis

Fe_3O_4 nanoparticles were prepared by a well-established chemical co-precipitation method.[31,32] A solution containing ferric (Fe^{3+}) chloride and ferrous (Fe^{2+}) sulfate was introduced into deionized water (Millipore, Direct-Q5, 18.2 MΩ cm). The mixture was stirred for an hour and oleic acid was added as a surfactant. The addition of base was carried out at 80 °C by maintaining the pH at 9–10. The formed nanoparticles were magnetically decanted and washed several times with deionized water to remove unwanted residual salt. The wet slurry was dispersed in kerosene and centrifuged at 12 000 rpm for 15 min to remove aggregates. The separated supernatant was labeled as ferrofluid.

MR fluid was prepared using Fe_3O_4 micron-sized (<5 μm) particles acquired from Sigma-Aldrich. The powder was mixed

with acetone for wet grinding at 400 rpm for five hours in a Retsch Co. Planetary ball mill. The weight to volume ratio of tungsten carbide (WC) balls and powder was maintained at 10 : 1 for effective grinding. MR fluid was prepared with a 30% volume fraction of ground Fe_3O_4 particles with a small amount of oleic acid added thereon as a surfactant and then dispersed in kerosene. The synthesized MRF was stirred and homogenized for half an hour. Thereafter, the MR fluid was mixed with different volume concentrations of ferrofluid: 5% (sample A), 10% (sample B) and 20% (sample C). These F-MRFs samples were ultrasonicated for 20 minutes, followed by heating at 60 °C for an hour (Fig. 1).

2.2 Characterization

The XRD patterns of the samples were recorded on a Rigaku powder X-ray diffractometer (Model XRG 2 kW) with a scanning rate of 0.02° s^{-1} and 2θ range from 20° to 70° at 40 kV and 30 mA automatic divergence slit system using Cu Kα radiation (λ = 1.54059 Å). The particle size and microstructure of particles were analyzed using a Tecnai HRTEM operated at 300 kV electron accelerating voltage. The magnetization measurements of FF and MRF were performed on a Lakeshore vibrating sample magnetometer (VSM, Model no. 7304). The rheological and viscoelastic properties of all the samples were investigated using an MCR-301 rheometer (M/s Anton Paar). A special plate–plate spindle, TG16-MRD, was employed for all the measurements. A coaxial magnetic field was applied in a perpendicular direction to the sample during the test. The gap between the measuring plate and the sample was always maintained, i.e. 0.3 mm for 0.3 mL ferrofluid. The visualization of chain dynamics was observed on a twice diluted F-MRF sample using a rheomicroscopy setup by applying a coplanar magnetic field. The rheomicroscopy setup consists of a CCD camera, objective, microscope tube and light source. The sample was illuminated from below. The equipment was warmed up for half an hour before the measurement and calibrated using a specified standard.
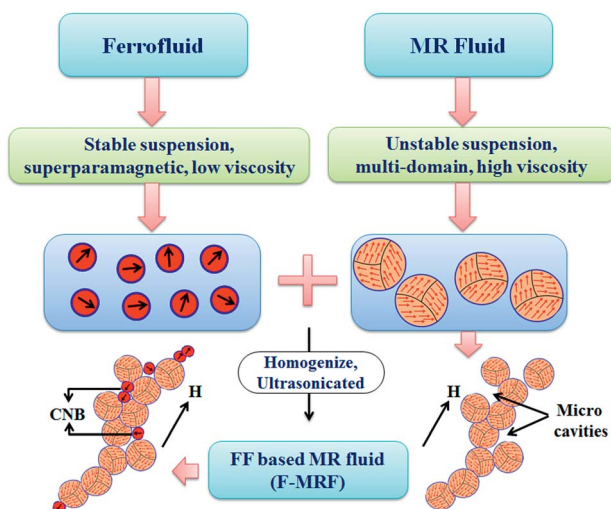
3. Results and discussion

3.1 Structural characterization

Fig. 2 shows the X-ray diffraction patterns of MRF and FF particles. The diffraction peaks and their intensity confirm the cubic spinel-type lattice characteristics of Fe_3O_4 (JCPDS card no: 19-629). It can be seen that sharp diffraction lines indicate the presence of larger-sized particles while broad diffraction peaks confirm the nanosized magnetite crystalline phase. The shape and size distribution of F-MRFs particles was examined by HRTEM and shown in Fig. 3. The finer particles, 10–15 nm, belong to FF whereas ∼250 nm particles correspond to MRF.

3.2 Magnetization measurement

The room temperature magnetisation measurements for FF and MR fluids are shown in Fig. 4(a) and (b), while insets (i) and (ii) exhibit the M–H curve for FF and MRF in powder form respectively. The FF system has no coercivity or remanence and does not saturate even at a field strength of 0.6 T, due to finite size effects,[33] and a maximum saturation magnetization of 46.8 emu g^{-1} was obtained for FF particles. However, MRF particles give a better response and saturate at a lower field strength compared to FF particles. For MRF particles, the values of saturation magnetization (M_s), remanence (M_r) and coercivity (H_c) were found to be 53.14 emu g^{-1}, 13.2 emu g^{-1} and 258.6 Oe, respectively. The magnetization of FF and MR fluids may be expressed using the following equation[34,35]

$$M = \int_0^\infty L(\alpha)f(D)d(D)$$

where $L(\alpha)$ is the Langevin function, $L(\alpha) = M_s^f\left(\coth(\alpha) - \dfrac{1}{\alpha}\right)$; $M_s^f = M_d\phi$ with $\alpha = \dfrac{M_dH\left(\frac{1}{6}\pi D^3\right)}{kT}$, $f(D)$ is the log-normal size distribution of MNPs, H is the applied magnetic field, k is the Boltzmann constant, T is the temperature, M_s^f is the fluid magnetization, ϕ is the solid volume fraction and M_d is the domain magnetization. It is assumed that the large particles experience a higher magnetic moment energy than smaller ones. Therefore, the larger-sized particles can be oriented easily

Fig. 1 Schematic view of preparation and role of ferrofluid nanoparticles in F-MRFs.
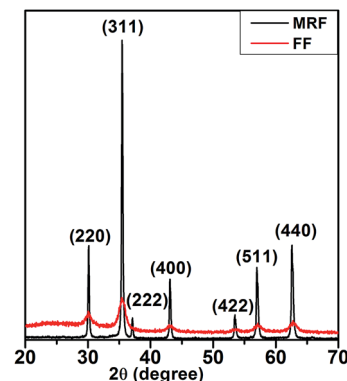

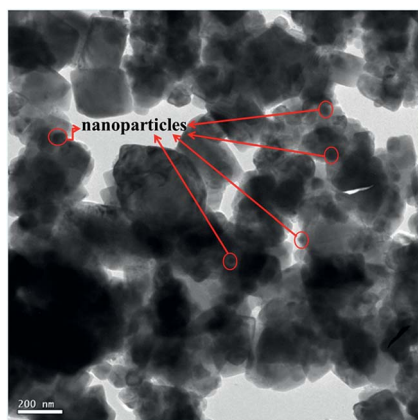Fig. 2 X-ray diffraction curve of FF and MRF samples.

Fig. 3   HRTEM image of F-MRF.

in the direction of a magnetic field and saturate much faster at low field strengths.

3.3   Rheological and viscoelastic measurements

3.3.1   Flow behaviour. The rheological measurements were carried out at room temperature. Fig. 5(a) shows the variation in viscosity with shear rate (0.1–1000 s^{-1}) for FF, MRF and sample 'C' with and without a magnetic field. In the absence of a magnetic field, FF shows Newtonian behaviour while the viscosity of MRF and sample 'C' decreases with increasing shear rate, exhibiting shear thinning. At a lower shear rate, a disordered arrangement of particles enhanced flow resistance. When the shear rate increased, particles started to arrange their orientation along the direction of shear, which led to a decrease in viscosity.[36] However, in the presence of a magnetic field, the viscosity of FF, MRF and sample 'C' increased and also demonstrated shear thinning behaviour. A similar trend has been observed for F-MRFs samples A, B and C. It is assumed that at low shear rate magnetically induced chain clusters sustain their existence due to dominant magnetic interactions while at high shear rate these structures break down and fluid starts to flow. In Fig. 5(a), it is remarkable to notice that the viscosity is increasing as the concentration of ferrofluid particles increases and it is a maximum for sample 'C' *i.e.* 20%
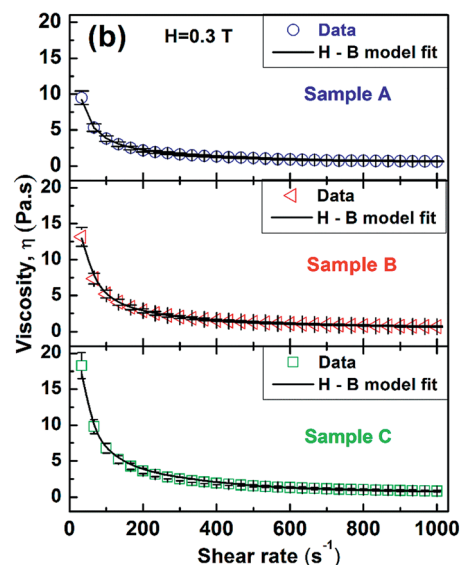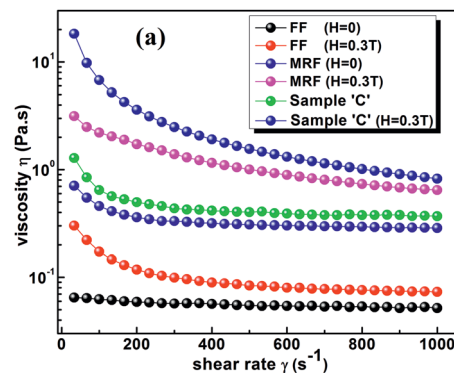
Fig. 5   (a) Variation in viscosity with shear rate with and without magnetic field for FF and MRF samples.(b) Conformity of experimental results with H−B model for F-MRFs samples.

ferrofluid nanoparticles.[17] The increase in viscosity is attributed to the occupancy of nanoparticles in microcavities formed among the micron-sized particles and also attached to the end of micron-sized particles due to dipole–dipole interactions forming a nanobridge.[21]
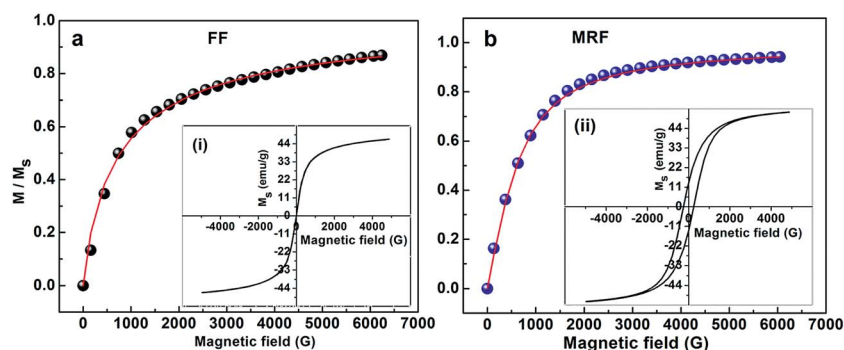

Fig. 4   Room temperature magnetization measurements of FF (a) and MRF samples (b). Inset (i) and (ii) M−H curves for FF and MRF in powder form, respectively.

The rheological behaviour of F-MRFs could be described using the H–B model,[36] *i.e.*

$$\tau = \tau_{H_0} + \tau_0 + k\dot{\gamma}^n$$

where τ_{H_0} and τ_0 are yield stresses with and without magnetic field respectively, τ is the shear stress, k is the consistency index, n is the shear-thinning exponent and $\dot{\gamma}$ is the shear rate. Fig. 5(b) indicates that the rheological measurements for samples A, B and C are in good agreement with this model. The term $k\dot{\gamma}^n$ shows the shear thinning behaviour of F-MRFs under the magnetic field. The values of the shear-thinning exponent (n) analysed from this model are 0.8, 0.72, and 0.7 for samples A, B and C respectively.

3.3.2 Magnetoviscous effect. Fig. 6 shows the magnetoviscous effect of F-MRFs. The viscosity increases on increasing the magnetic field intensity due to dipole–dipole interaction among the magnetic particles and the formation of chain-like structures in the direction of the magnetic field. The magnetic dipole moment of a particle is given by $\mu = V\chi H$, where $V = \pi d^3/6$, *i.e.* the volume of the particle, d is the diameter of the particle, χ is the magnetic susceptibility of the particle and H is the applied magnetic field. Fig. 7 shows the rheomicroscopic view of cluster formation in a twice diluted F-MRF sample under a magnetic field of ~500 G. These long chains provide a hindrance to the free flow of fluid thereby resulting in increased viscosity. The formation of aggregates is opposed by Brownian dispersion, and the field-induced aggregation *versus* Brownian dispersion can be expressed as a coupling constant,

$$\lambda = \frac{\pi(\mu_0\chi H)^2 d^3}{18 k_B T}$$

where μ_0 and H are the permeability of free space and the magnitude of the applied magnetic field, respectively. T and k_B are the absolute temperature and Boltzmann constant. For $\lambda \gg 1$, aggregation is highly favoured and commonly occurs in MR fluids.[37] While for $\lambda \ll 1$, dispersion is favoured and is used as a design parameter for the ferrofluid.[1] Due to the presence of micron-sized magnetic particles in the ferrofluid
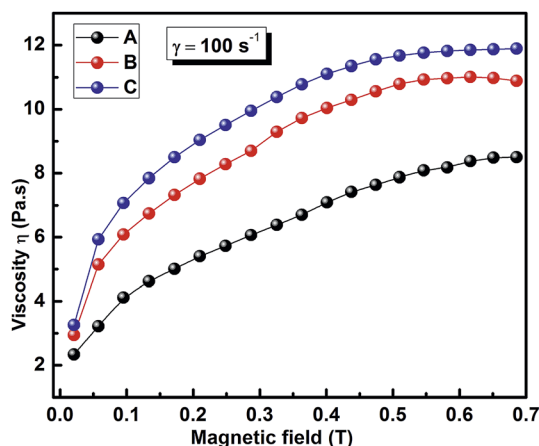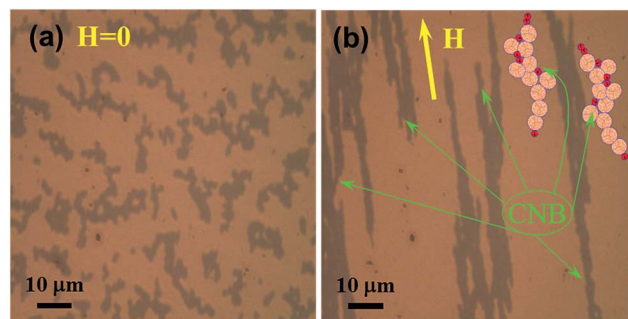

Fig. 7 Rheomicroscopy image of twice diluted F-MRF (sample A) (a) without magnetic field, (b) formation of chain-like structures and CNBs in presence of magnetic field (~500 G).

the aggregation parameter is calculated for a nanosized magnetite sphere by

$$\lambda = \frac{\mu_0 M_s H \pi d^3}{6 k_B T}$$

where $\mu_0 M_s$ is the saturation magnetization of the particles. The coupling parameter λ is the key parameter that determines the equilibrium suspension of chain-like structures of magnetic particles. The value of λ for micron-sized particles is much higher (~95.4) as compared to nanosized particles (~1.5), which reveals that the dipolar interaction among the varying-sized particles plays a dominant role in cluster formation. Thus, these flexible chains grow with the increase in concentration and further strengthening of the applied magnetic field.

3.3.3 Field-induced relaxation behavior. A time-dependent viscosity measurement was performed to study the relaxation behavior in samples A, B, C and the results are shown in Fig. 8. In this figure three regions can be considered as (I) magnetic field OFF, (II) magnetic field ON and (III) magnetic field OFF. At the boundary of regions I and II is shown the formation of magnetically induced chain structures leading to an increase in viscosity due to enhanced dipolar interaction. On the removal of the magnetic field, the viscosity decreases due to shear forces dominating, which destroyed the magnetically induced chain-like structures. However, the viscosity in region III is greater than the initial viscosity in region I. This indicates that part of the structures formed have not been destroyed or new aggregates have been re-established. The decrease of viscosity with time in region III (inset of Fig. 8) is related to the gradual distortion of aggregate structures *i.e.* breaking of CNBs as shown in the schematic for Fig. 8, which indicates that magnetic particles retain some memory of the applied magnetic field.[33,38]

3.3.4 F-MRFs figures of merit. There are several figures of merit which are related to the fluid efficiency and defined as a ratio of the mechanical to the electrical power densities of a MR fluid-based device. Fig. 9(a) shows the first figure of merit $F_1 = \tau^2/\eta$ as a function of shear rate. It reveals the dynamic range of the MR devices as well as the required MR fluid volume and power consumption.[30] A significant improvement in F_1 shows a shear-thinning behavior of the fluids on increasing

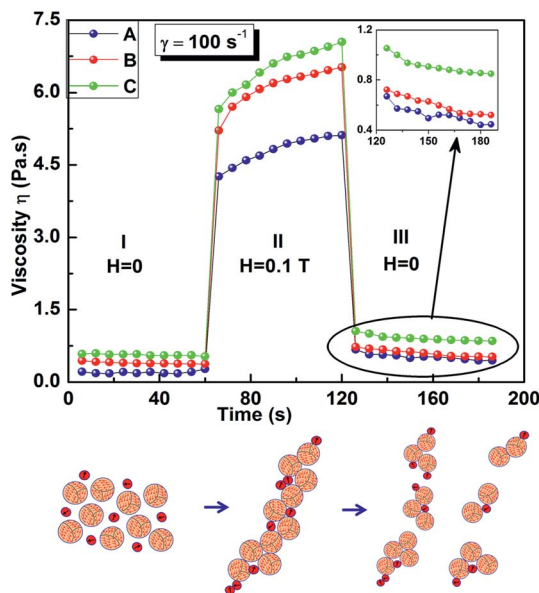**Fig. 6** Magnetoviscous effect of F-MRF samples.

Fig. 8 Viscosity of samples A, B and C *versus* time at shear rate 100 s^{-1}, region I: magnetic field $H = 0$, region II: magnetic field $H = 0.1$ T and region III: magnetic field $H = 0$ and schematic view of formation and destruction of chain-like structures.

Fig. 10 (a) storage (G') and (b) loss modulus (G'') as a function of shear strain at a magnetic field of 0.3 T. (c) Loss factor as a function of magnetic field strength for samples A, B and C.

nanoparticle concentration. Also, the figure of merit $F_2 = \tau^2/\eta\rho$ as a function of shear rate is shown in Fig. 9(b). This figure of merit is similar to F_1 except it is related to density and shows a small vertical change in the data. In general, both F_1 and F_2 exhibit better rheological behavior due to shear thinning at high shear rate. By comparing this figure of merit, the stability of sample 'C' seems to improve on pure MRF samples A and B at higher shear rates. Hence, it is found that the effect of small-sized particles in MRF plays a vital role in its stability.

3.3.5   Strain amplitude and magneto sweep measurements. The storage or elastic modulus (G') and loss or viscous modulus (G'') were determined as a function of shear strain at applied magnetic field $H = 0.3$ T and frequency $\omega = 10$ rad s^{-1}. Fig. 10(a) and (b) show that all the samples have a similar pattern during the strain sweep test. The elastic response (G') is stronger than the viscous one (G''), indicating the existence of strong links between the particles that form the microscopic structure of the
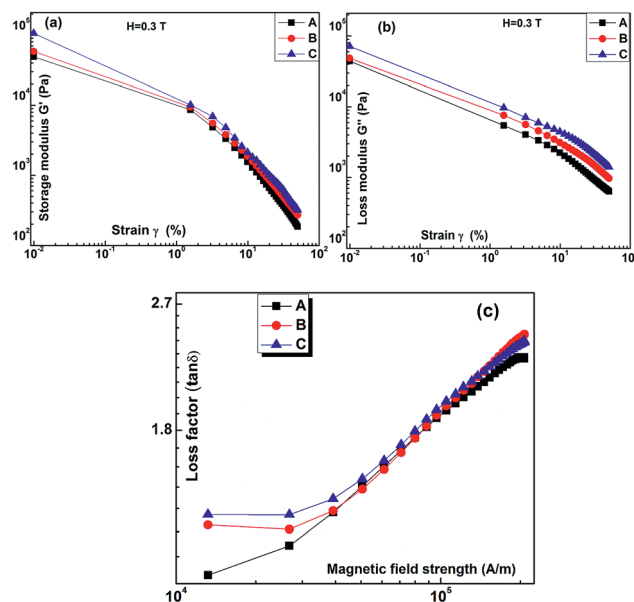
suspensions.[39] However, the storage modulus increases with increasing weight fraction of nanosized particles, which indicates the enhanced interaction and formation of chain-like clusters. The loss factor (ratio of G'' and G') as a function of magnetic field strength is shown in Fig. 10(c). This further indicates that magnetic interactions induce the formation of chains between nanosized and micron-sized particles.

4.   Conclusion

Bidispersed F-MRFs with varying volume percentages of ferro-fluid nanoparticles have been synthesized and investigated for their structural, magnetic, magnetoviscous and viscoelastic properties. It is believed that the incorporation of nanosized particles in MR fluid provides better stability and an enhancement in viscosity with an increase in the number density of particles. Addition of nanoparticles to MR suspension initiates the formation of strong chain-like clusters by filling
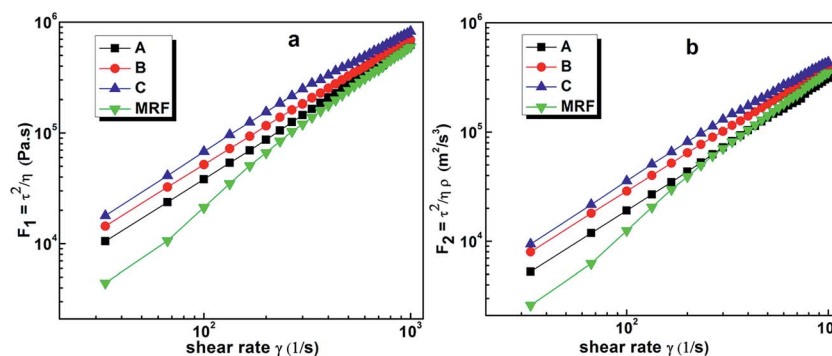

Fig. 9 Figures of merit (a) F_1 and (b) F_2 as a function of shear rate for samples A, B and C at magnetic field = 0.3 T.

microcavities created among the larger particles and the existence of these structures was confirmed by rheomicroscopy. Several figures of merit for F-MRFs-based devices were also compared in terms of fluidity at high shear rate and also proved to be stable. The storage or elastic modulus (G') and the loss or viscous modulus (G'') were determined as a function of the shear strain and results show that $G' > G''$. The Herschel–Bulkley model was used to characterize the rheological behavior of F-MRFs.

Acknowledgements

References

1 R. E. Rosenzweig, *Ferrohydrodynamics*, Cambridge University Press, 1985.

2 R. G. Larson, *The structure and rheology of complex fluids*, Oxford university press, New York, 1999.

3 G. Bossis, O. Volkova, S. Lacis and A. Meunier, *Magnetorheology: fluids, structures and rheology, Ferrofluids*, Springer, 2003, pp. 202–230.

4 S. Odenbach, *Magnetoviscous effects in ferrofluids*, Springer-Verlag, Berlin Heidelberg, 2002.

5 S. E. Premalatha, R. Chokkalingam and M. Mahendran, Magneto Mechanical Properties of Iron Based MR Fluids, *Am. J. Polym. Sci.*, 2012, **2**, 50–55.

6 P. F. Luckham and M. A. Ukeje, Effect of particle size distribution on the rheology of dispersed systems, *J. Colloid Interface Sci.*, 1999, **220**, 347–356.

7 J. de Vicente, J. D. Durán and A. V. Delgado, Electrokinetic and viscoelastic properties of magnetorheological suspensions of cobalt ferrite, *Colloids Surf., A*, 2001, **195**, 181–188.

8 M. Hong, B. Park and H. Choi, Preparation and characterization of MR fluid consisting of magnetite particle coated with PMMA, *J. Phys.: Conf. Ser.*, 2009, 012055.

9 M. T. Lopez-Lopez, G. Vertelov, G. Bossis, P. Kuzhir and J. D. G. Duran, New magnetorheological fluids based on magnetic fibers, *J. Mater. Chem.*, 2007, **17**, 3839–3844.

10 I. Bica, The obtaining of magneto-rheological suspensions based on silicon oil and iron particles, *J. Mater. Sci. Eng. B*, 2003, **98**, 89–93.

11 S. Singamaneni, V. N. Bliznyuk, C. Binek and E. Y. Tsymbal, Magnetic nanoparticles: recent advances in synthesis, self-assembly and applications, *J. Mater. Chem.*, 2011, **21**, 16819–16845.

12 M. T. López-López, A. Gómez-Ramírez, J. D. Durán and F. González-Caballero, Preparation and characterization of iron-based magnetorheological fluids stabilized by addition of organoclay particles, *Langmuir*, 2008, **24**, 7076–7084.

13 K. Shah, M.-S. Seong, R. Upadhyay and S.-B. Choi, A low sedimentation magnetorheological fluid based on plate-like iron particles, and verification using a damper test, *Smart Mater. Struct.*, 2014, **23**, 027001.

14 J. de Vicente, D. J. Klingenberg and R. Hidalgo-Alvarez, Magnetorheological fluids: a review, *Soft Matter*, 2011, **7**, 3701–3710.

15 N. Rosenfeld, N. M. Wereley, R. Radakrishnan and T. S. Sudarshan, Behavior of magnetorheological fluids utilizing nanopowder iron, *Int. J. Mod. Phys. B*, 2002, **16**, 2392–2398.

16 R. Patel and B. Chudasama, Hydrodynamics of chains in ferrofluid-based magnetorheological fluids under rotating magnetic field, *Phys. Rev. E: Stat., Nonlinear, Soft Matter Phys.*, 2009, **80**, 012401.

17 N. Wereley, A. Chaudhuri, J.-H. Yoo, S. John, S. Kotha, A. Suggs, R. Radhakrishnan, B. Love and T. Sudarshan, Bidisperse magnetorheological fluids using Fe particles at nanometer and micron scale, *J. Intell. Mater. Syst. Struct.*, 2006, **17**, 393–401.

18 P. P. Phulé and J. M. Ginder, Synthesis and properties of novel magnetorheological fluids having improved stability and redispersibility, *Int. J. Mod. Phys. B*, 1999, **13**, 2019–2027.

19 M. López-López, J. De Vicente, G. Bossis, F. González-Caballero and J. Durán, Preparation of stable magnetorheological fluids based on extremely bimodal iron–magnetite suspensions, *J. Mater. Res.*, 2005, **20**, 874–881.

20 M. Hagenbüchle and J. Liu, Chain formation and chain dynamics in a dilute magnetorheological fluid, *Appl. Opt.*, 1997, **36**, 7664–7671.

21 R. Patel, Mechanism of chain formation in nanofluid based MR fluids, *J. Magn. Magn. Mater.*, 2011, **323**, 1360–1363.

22 K. Butter, P. Bomans, P. Frederik, G. Vroege and A. Philipse, Direct observation of dipolar chains in iron ferrofluids by cryogenic electron microscopy, *Nat. Mater.*, 2003, **2**, 88–91.

23 L. A. Powell, W. Hu and N. M. Wereley, Magnetorheological fluid composites synthesized for helicopter landing gear applications, *J. Intell. Mater. Syst. Struct.*, 2013, **24**, 1043–1048.

24 D. Baranwal and D. T. Deshmukh, MR-Fluid Technology and Its Application-A Review, *International Journal of Emerging Technology and Advanced Engineering*, 2012, **2**.

25 K. Gudmundsson, F. Jonsdottir, F. Thorsteinsson and O. Gutfleisch, An experimental investigation of unimodal and bimodal magnetorheological fluids with an application in prosthetic devices, *J. Intell. Mater. Syst. Struct.*, 2011, **22**, 539–549.

26 M. Kciuk and R. Turczyn, Properties and application of magnetorheological fluids, *Journal of Achievements in Materials and Manufacturing Engineering*, 2006, **18**, 127–130.

27 B. J. Park, F. F. Fang and H. J. Choi, Magnetorheology: materials and application, *Soft Matter*, 2010, **6**, 5246–5253.

28 A.-G. Olabi and A. Grunwald, Design and application of magneto-rheological fluid, *Mater. Des.*, 2007, **28**, 2658–2664.

29 W. Kordonski and D. Golini, Multiple application of magnetorheological effect in high precision finishing, *J. Intell. Mater. Syst. Struct.*, 2002, **13**, 401–404.

30 M. R. Jolly, J. W. Bender and J. D. Carlson, Properties and applications of commercial magnetorheological fluids, *J. Intell. Mater. Syst. Struct.*, 1999, **10**, 5–13.

31 Z. Wang and C. Holm, Structure and magnetic properties of polydisperse ferrofluids: A molecular dynamics study, *Phys. Rev. E: Stat., Nonlinear, Soft Matter Phys.*, 2003, **68**, 041401.

32 A. Shankar, M. Chand, S. Kumar, V. Singh, G. Basheed, S. Thakur and R. P. Pant, Spin resonance investigations on water-based magnetite ferrofluid, *Magnetohydrodynamics*, 2013, **49**, 310–316.

33 M. Chand, S. Kumar, A. Shankar, R. Porwal and R. P. Pant, The size induced effect on rheological properties of Co-ferrite based ferrofluid, *J. Non-Cryst. Solids*, 2013, **361**, 38–42.

34 R. Upadhyay, K. Parekh and R. Mehta, Spin-glass transition in a model magnetic fluid: electron spin resonance investigation of $Mn_{0.5}Zn_{0.5}Fe_2O_4$ nanoparticles dispersed in kerosene, *Phys. Rev. B: Condens. Matter Mater. Phys.*, 2003, **68**, 224434.

35 A. O. Ivanov and O. B. Kuznetsova, Magnetic properties of dense ferrofluids: an influence of interparticle correlations, *Phys. Rev. E: Stat., Nonlinear, Soft Matter Phys.*, 2001, **64**, 041405.

36 R. Hong, Z. Ren, Y. Han, H. Li, Y. Zheng and J. Ding, Rheological properties of water-based Fe_3O_4 ferrofluids, *Chem. Eng. Sci.*, 2007, **62**, 5912–5924.

37 S. Samouhos and G. McKinley, Carbon nanotube–magnetite composites, with applications to developing unique magnetorheological fluids, *J. Fluids Eng.*, 2007, **129**, 429–437.

38 E. Ghasemi, A. Mirhabibi and M. Edrissi, Synthesis and rheological properties of an iron oxide ferrofluid, *J. Magn. Magn. Mater.*, 2008, **320**, 2635–2639.

39 K. Shah, J.-S. Oh, S.-B. Choi and R. Upadhyay, Plate-like iron particles based bidisperse magnetorheological fluid, *J. Appl. Phys.*, 2013, **114**, 213904.